Back to Belgium Grants

Final Report

Name of the researcher	dr. Mihail D. Croitoru
Selection Year	2012
Host institution	University of Antwerp
Head of the CMT group	Prof. dr. F. Peeters
Period covered by this report	from 01/09/2013 to 31/08/2015
Title of the project	**Novel confinement-induced phenomena in superconducting nanograins**

1. Objectives of the proposal (1 page)

Superconducting correlations in metallic nanograins coupled to a phonon bath: Over the last 50 years the properties of nanoscale superconductors have been investigated extensively, both theoretically and experimentally, due to their general importance for the understanding of the nature of the ground state in confined systems. Furthermore, the question of how the superconducting properties of confined systems are altered with thickness down to the nanometer size range has also significant technological ramifications. Anderson argued that conventional superconductivity should disappear for sample sizes such that the average level spacing is of the order of the BCS gap Δ. Above the Anderson limit the critical temperature *Tc* should exhibit quantum oscillations with thickness dependent resonant enhancements as it was predicted by Blatt and Thomson. However, subsequent experimental studies of superconducting confined systems showed either a decrease or an increase of *Tc* with sample thickness, depending on the material. An overview of the experimental findings over the last 50 years shows that *Tc* decreases as the strength of the *e-ph* interaction increases.

The purpose of the investigation was to check within the framework of BCS theory of superconductivity or beyond it the idea that the experimental results can be explained by interplay of quantum confinement for the electronic degrees of freedom and a dissipative environment due to electron-(bulk) phonon interaction.

Peculiarities of the orbital effect in the FFLO state in quasi-1D SCs: The discovery of a series of new superconducting compounds with unique properties in magnetic field and pronounced reduced dimensionality has stirred up considerable interest in the subject of the Fulde-Ferell-Larkin-Ovchinnikov (FFLO) phase. Notable examples include the quasi-1D organic Bechgaard salts (TMTSF)2*X*, where anion *X* is PF6, ClO4, etc., polysulfur nitride (SN*x*), the metal-chalcogenidebased compounds, transition-metal carbides, the quasi-1D *M*2Mo6Se6 compounds (relatives of the quasi-3D Chevrel phases), lithium purple bronze, and arrays of 4A superconducting carbon nanotubes embedded in the linear pores channels of AFI zeolite single crystals. The high crystallographic quasi-1D structure of these compounds and high values of the Maki parameter convert them into prime candidates for the search of the Fulde-Farrel-Larkin-Ovchinnikov state. Moreover, it has been shown within the layered SC model under the applied in-plane magnetic field in the FFLO phase that the experimentally observed anomalous field-direction dependence of the upper critical field as well as the anomalous cusps in this dependence due to resonances between the modulation wave vector and the vector potential can serve as a direct evidence for the appearance of the FFLO phase in layered superconductors.

The aim of this work was to investigate the possibilities of the spatially modulated superconducting phase formation in quasi- 1D superconductors with *s*-wave pairing.

Coherent dynamics of confinement induced multiband superconductors: Recently the experimental observation of the amplitude / Higgs mode in conventional BCS SCs has been reported. By using monocycle-like THz pulse and the sample with small gap energy, the non-adiabatic excitation conditions have been realized. The observed oscillation frequencies were in excellent agreement with the asymptotical values of the bulk gap energy as was previously theoretically predicted. However, the power law decay index was observed to have values larger than one depending on the pump intensity. In my recent work I have studied the effect of energy-dependent electronic density of states in the proximity of the Fermi level on the Higgs mode. It was found that non-adiabatic dynamics of the shallow-band superconductors is qualitatively different from its bulk counterpart. Landau damped dephased oscillations occur on average faster in a nanoscale system. The power law changes from 1/2 in the bulk and non-resonant case to 3/4 for superconductors with resonant widths.

The aim of this work was to investigate (*i*) how the intrinsic multiband nature of the nanoscale superconductors can modify the coherent dynamics of pairing induced by a non-adiabatic perturbation; (*ii*) The Higgs amplitude mode of the order parameter of an ultracold confined Fermi gas in the BCS regime after a quench of the coupling constant.

Confinement-induced ferroelectricity in ultra-small SC grains: The recent experiment showed that cold clusters may attain anomalous electric dipole moments at very small temperatures. In contrast, room-temperature measurements show normal metallic polarizabilities. It is found that generally, transition temperature decreases as cluster size increases, with pronounced even-odd alternations.

Within the project it was necessary to proof that this new state of metallic matter is related to the fact that the spatial distribution of the pair condensate is strongly nonuniform in metallic clusters. Since the positive ion charge is evenly distributed, the formation of strongly nonuniform pair condensate in metallic grains induces electric multipole moments, which can be detected in experiments.

2. Methodology in a nutshell (1 page)

The general Hamiltonian for a coupled electron-phonon system interacting via a linear interaction is given by

$$H = \sum_{\mathbf{p},\sigma} \varepsilon_p a^\dagger_{p,\sigma} a_{p,\sigma} + \sum_{\mathbf{w}} \omega_{\mathbf{w}} \left(b^\dagger_{\mathbf{w}} b_{\mathbf{w}} + \tfrac{1}{2}\right) + \sum_{\mathbf{w},\mathbf{p},\sigma} V_{\mathbf{w}} a^\dagger_{\mathbf{p}-\mathbf{w},\sigma} a_{\mathbf{p},\sigma} \left(b_{\mathbf{w}} - b^\dagger_{-\mathbf{w}}\right)$$

Here *p* is integer numbering the single-particle energy levels ε_p, the operator $a_{p,\sigma}$ annihilates an electron in state *p* with spin σ and the operator b_w annihilates a phonon in state w. We describe the phonons by a Debye spectrum, i.e., we use $\omega_w = c|w|$, where *c* denotes the velocity of sound and w ranges from zero to w_D, the Debye wave number. The corresponding maximum phonon energy is denoted by ω_D. Here coupling V_w is related with the *e-ph* coupling used in superconductivity as

$$\lambda = \frac{2V_w^2 N(0)}{\omega_w}$$

where $N(0) = \frac{m_e k_F}{2\pi^2\hbar^2}$. Here k_F denotes the Fermi wave vector. For our quantitative studies performed within this project we have used bulk phonon parameters, thus neglecting any change of the phonon spectrum due to the presence of the surface. This approach is motivated by the large ratio of electron and phonon quantum-confinement energies which scale as m_{ion}/m_e.

To describe the superconducting state we consider the reduced Bardeen-Cooper-Schrieffer (BCS) pairing Hamiltonian, where only the time-reversal states are paired

$$\widehat{H}_{\mathrm{BCS}} = \sum_{p,\sigma} \varepsilon_p a^\dagger_{p,\sigma} a_{p,\sigma} - \sum_{p,q} g_{pq} a^\dagger_{p\uparrow} a^\dagger_{p\downarrow} a_{q\downarrow} a_{q\uparrow}$$

where the interaction matrix element g_{qp} is given by

$$g_{qp} = g \int \mathrm{d}^3 r \, |\varphi_q(\mathbf{r})|^2 |\varphi_p(\mathbf{r})|^2$$

with *g* denoting the coupling constant and $\varphi_q(\mathbf{r})$ the single-electron wave function. The first term in the BCS Hamiltonian contains the single- electron energies, and the second term is the attractive (when $g > 0$) pairing interaction due to the exchange of virtual phonons. In the bulk the real inter-electron potential is well approximated by a δ-function pseudopotential. Employing such a simplified interaction requires a regularization, which makes the matrix elements non-zero only between states within the Debye window around the Fermi surface.

3. Results (8-10 pages)

3.1. Superconducting correlations in metallic nanograins coupled to a phonon bath: Making use of the general theory described in the section "Methodology in a Nutshell" and taking into account the phonon induced contribution to the level broadening, which can be expressed in terms of the spectral Eliashberg function

$$\Gamma(\xi;T) = 2\pi\hbar \int_0^{\omega_D} d\omega' \alpha^2 F(\omega') \left[1 - f(\xi - \hbar\omega') - 2n(\hbar\omega') - f(\xi - \hbar\omega')\right]$$

where $f(\xi)$ and $n(\hbar\omega')$ are the electron and phonon occupation numbers, respectively. With increasing sample size the energy separation between different single-electron levels decreases and more levels move into the Debye window, thereby opening additional inter-level scattering channels. Therefore, the use of 3D acoustic (LA) e-ph scattering should be adequate for calculations of the acoustic phonon-induced single-electron level broadening when the average energy spacing $\delta \approx 2\pi^2\hbar^2/m_e k_F V$ is sufficiently smaller than the mean LA phonon energies. Here V is the sample volume. Within the 3D Debye model the Eliashberg function is $\alpha^2 F(\omega) = \lambda(\omega/\omega_D)^2\theta(\omega_D-\omega)$, which results at $T = 0$ in the simplified expression for the level broadening used in the calculations (see for details, the manuscript of the article).

In the case of finite superconducting systems the mean field approximation exhibits several drawbacks. The most evident is the presence of sharp phase transitions, which is characteristic of very large systems. This effect is due to statistical fluctuations. The static-path approximation (SPA) provides a microscopic way to include the static fluctuations of the mean field. SPA considers only the static paths in the path integral representation of the partition function. In this work we have used the reduced SPA formalism within which we obtained the equation for the pairing gap

$$\Delta_p - \Delta_p^P = \frac{1}{2} g k_B T / \Delta_p$$

and equation for the density gap

$$\Delta_p^P = \sum_q \frac{g_{p,q}\Delta_q}{2E_q} \int_0^{\omega_D} d\xi \frac{F(\xi_q - \xi, \Gamma_q)}{2E_q(\xi)} \tanh\left(\frac{E_q}{2k_B T}\right)$$

where E_q is the quasi-particle energy given by $E_q(\xi) = \sqrt{[\xi_q(\lambda) - g/2]^2 + |\Delta_q|^2}$ within the pairing interval (Debye window) and $E_q(\xi) = |\,\xi_q(\lambda)\,|$ outside. Here $\Delta_q = \int dr |\,\varphi_q(\mathbf{r})\,|^2\Delta(r)$, $\Gamma_q = \Gamma(\xi_q(\lambda);T)$ is the total width of the q-level, which is approximated by the phonon contribution, and the single electron spectrum is described by $\xi_q(\lambda) = \mu + (\varepsilon_q^0 - \mu)/(1 + \lambda)$ with $\varepsilon_q^0 = \hbar^2 k_q^2/2m_e$. This expression takes into account the modification of the single-electron spectrum due to the electron-phonon interaction, tied to a thin energy shell of approximate width $2\hbar\omega_D$. The function $F(\xi_q(\lambda) - \xi, \Gamma_q)$ describes the shape of the broadened levels. If one also assumes that $F(\xi_q(\lambda) - \xi, \Gamma_q) = \theta(\Gamma_q - |\xi_q - \xi|)/2\Gamma_q$, where $\theta(x)$ is the Heaviside step function, then the integral can be done analytically (for $T \to 0$) and we obtain the pairing gap equation used in the calculations

$$\Delta_p^P = -\sum_q \frac{g_{p,q}\,\Delta_q}{2\Gamma_q} \ln \frac{\xi_q + \Gamma_q + \sqrt{(\xi_q + \Gamma_q)^2 + \Delta_q^2}}{\xi_q - \Gamma_q + \sqrt{(\xi_q - \Gamma_q)^2 + \Delta_q^2}}$$

The calculations were performed with parameters typical for aluminum, tin, niobium, and lead. Fig. 1 illustrates our results for the normalized reduced critical temperature, $T_C(\alpha)/\,T_C^B$, as a function of the sample size for aluminum, tin, niobium and lead metallic nanoparticles. Here T_C^B is the superconducting onset temperature for a sample with $D \to \infty$. For each sample size the transition temperature, $T_C(\alpha)$/, was defined as the temperature which corresponds to steepest descent of the superconducting order parameter. The order parameter takes into account thermal fluctuations on the level of reduced static-path approximation (SPA) or effective BCS. All our numerical results exhibit a feature typical for the size-dependent pairing in high-quality superconducting particles: $T_C(\alpha)$ fluctuates with sample size. The amplitude of the fluctuations increases with decreasing *e-ph* coupling. Qualitatively, the fluctuations of $T_C(\alpha)$ can be understood as follows. The pair correlations are non-zero only within a finite range marked by the Debye window around the chemical potential, μ. Moreover, the main contributions to the sum in the last equation come from states in the vicinity of the Fermi level. When varying the size of the grain, the number of states in the Debye window changes. The smaller the grain, the smaller the number of relevant states contributing to the pair correlations. However, because of the enhanced broadening of the single-electron levels in materials with stronger *e-ph* coupling, the $T_C(\alpha)$ fluctuations are weaker in these nanoparticles.

The solid curves in Fig. 1 are a guide for the eye and give the average size dependence of T_C in the range of grain widths D = 8 - 28 nm. For aluminum and tin nanoparticles we observe an overall increase of T_C by a factor of 2 in the case of aluminum and by a factor of 1.4 in the case of tin when decreasing D from bulk to $D \approx$ 8 nm. In contrast, the size dependencies of T_C are almost absent for niobium nanoparticles down to $D \approx$ 8 nm. The transition temperature shows a slight decrease of 4% when the width of the sample is decreased from $D \approx$ 30 nm to $D \approx$ 8 nm. A further reduction of the particle size leads to a slight increase of T_C before its suppression. Lead nanoparticles exhibit a small decrease of T_C with decreasing sample size. The transition temperature decreases by 3 - 4% when the width of the sample is decreased from $D \approx 30$ nm to $D \approx 8$ nm. The different behavior of Nb and Pb nanoparticles as compared with Al and Sn is a direct consequence of the fact that quantum confinement is smaller due to (*i*) the heavier electron mass and (*ii*) larger broadening of the single electron levels, both as a result of the stronger electron-phonon interaction.

Therefore in this work we showed how environmental entanglement emerges in the ground-state of the considered systems and why it has a strong influence on the superconducting characteristics. The pair-breaking effect due to thermal phonons was accounted for, which broadens the single electron levels, as well as the virtual phonons that renormalize the band electron mass. Without such level broadening and mass renormalization T_C always increases with decreasing sample size above the Anderson limit. In our theory, as corroborated by experimental observations, quantum confinement can either increase or show constant behavior/slight decrease of the average superconducting critical temperature, depending on the material parameters. Our analysis conclusively shows that a slight decrease of T_C for smaller samples is expected for the strongly phonon-coupled nanoparticles of lead while an increase is typical for samples made of weakly phonon coupled superconducting materials, both in accordance with experimental findings.

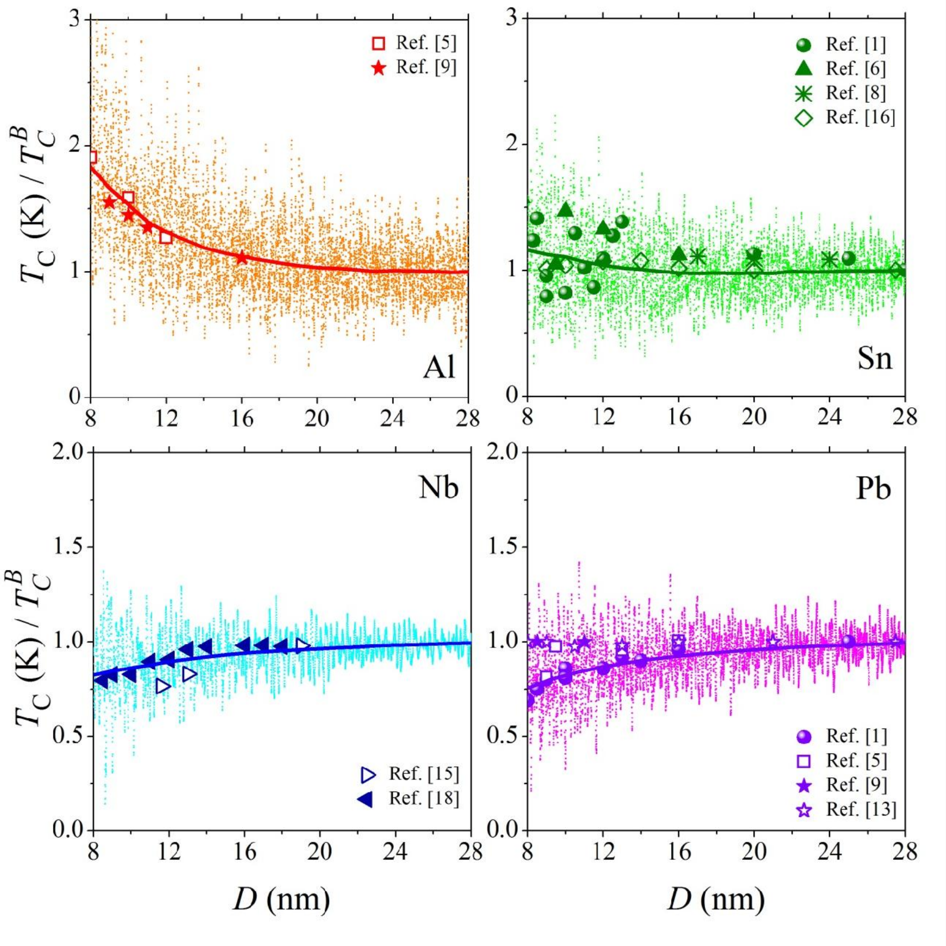

Fig. 1: Calculated variation of T_C with the sample size D for Al, Sn, Nb, and Pb nanograins. The solid curves give the average dependence. The large symbols show the experimental results.

We note that in the presence of disorder the level broadening can be size-dependent, because the effect of disorder typically increases with the reduction of sample size due to e.g. surface-roughness, resulting in a stronger level broadening at small sizes. Disorder also results in a repulsion of the energy levels in small metallic samples making them evenly distributed, which additionally decreases T_C when reducing the sample size. As was found by Altshuler and Aronov the Coulomb interaction combined with impurity scattering produces a dip in the density-of-states at the Fermi level that in turn further decrease the transition temperature with decreasing sample size. To estimate the effect of disorder we use a weak disorder model for homogeneous superconducting samples established by Finkelstein, according to which the suppression of superconductivity is driven by impurities that reinforce Coulomb and spin interactions. According to this model the critical temperature is found from the following expression

$$T_c = T_{c0} e^{-\frac{1}{\gamma}} \left(\frac{\gamma + t/4 - \sqrt{t/2}}{\gamma + t/4 + \sqrt{t/2}} \right)^{\frac{1}{\sqrt{2t}}}$$

Within this model we obtain the results shown as dashed lines in Fig. 1. For the calculations we adopted the following parameters R_S(Al) = 14.1 Ω, R_S(Sn) = 54 Ω, R_S(Pb) = 110 Ω, R_S(Nb) = 90 Ω.

Acknowledgement: The performed investigation required a large amount of numerical calculations. To pay tribute to the computational demand given by the above described problem I have used the cluster computational facilities available at the University of Bayreuth.

I acknowledge the fruitful collaboration and discussions with A. V. Vagov (Institute of Theoretical Physics III, University of Bayreuth, Germany), A. A. Shanenko (University of Pernambuco, Brazil), V. Z. Kresin Lawrence Berkeley National Laboratory, Berkeley, CA USA), V. N. Gladilin (Catholic University of Leuven, Belgium), S. N. Klimin (University of Antwerp, Belgium).

3.2. Coherent dynamics of confinement induced multiband superconductors: Coherent dynamics of nanoscale conventional superconductors was treated within the framework of the mean-field approximation. The basis equations were obtained after the Bogoliubov transformation of the Hamiltonian of the system interacting with an external field, $H = H_{SC} + H_{EM}$. The system Hamiltonian took the form

$$H_{\mathrm{SC}} = \sum_{\chi} R_{\chi} \sum_{\sigma} \gamma^{\dagger}_{\chi,\sigma}(t)\, \gamma_{\chi,\sigma}(t) + \sum_{\chi} \left[C_{\chi} \gamma_{\chi\uparrow}(t)\, \gamma_{\bar{\chi}\downarrow}(t) + C^{*}_{\chi} \gamma^{\dagger}_{\chi\uparrow}(t)\, \gamma^{\dagger}_{\bar{\chi}\downarrow}(t) \right] + E_g$$

with $E_g = 2 \sum_{\chi} \xi_{\chi} |v_{\chi}|^2$ and (in the Anderson approximate solution)

$$R_{\chi} = \frac{\xi_{\chi}^2 + \Delta_{\chi,0} \mathrm{Re}\left[\Delta_{\chi}(t)\right]}{E_{\chi}}, \quad C_{\chi} = \frac{\xi_{\chi}}{E_{\chi}} \left\{ \mathrm{Re}\left[\Delta_{\chi}(t)\right] - \Delta_{\chi,0} \right\} + i \mathrm{Im}\left[\Delta_{\chi}(t)\right]$$

Here $E_{\chi} = \sqrt{\xi_{\chi}^2 + |\Delta_{\chi,0}|^2}$ is the quasiparticle energy, ξ_{χ} is the single-electron energy counted from the Fermi level μ, Δ_{χ} is the current time dependent value of the order parameter, averaged on the χ-th wave function, while $\Delta_{\chi,0}$ is the value of the order parameter, for which the diagonalasing transformation of the Hamiltonian was done. H_{EM} is the Hamiltonian describing the coupling of the system to an external electro-magnetic field. The BdG equations are solved to provide for the particle-like and hole-like quasiparticle amplitudes $u_{\chi}(\mathbf{r})$ and $v_{\chi}(\mathbf{r})$ with excitation energy $E_{\chi} > 0$. H_e is the single-particle Hamiltonian.

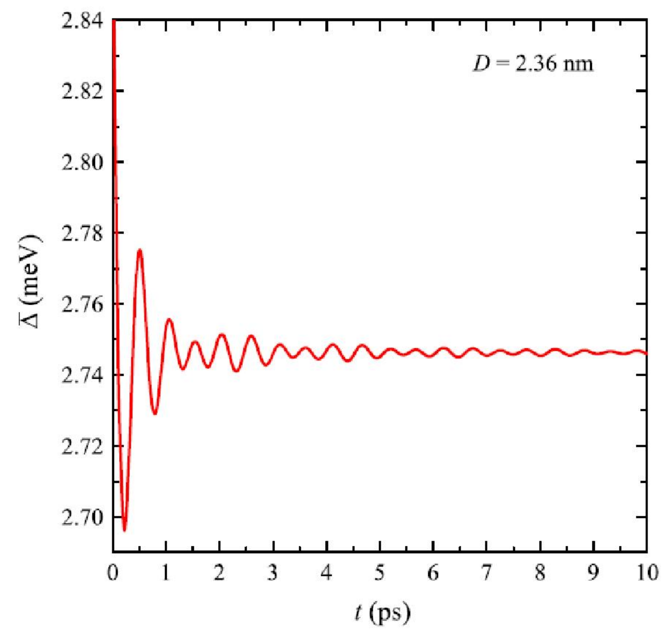

Fig. 2: Time evolution of the order parameter for a wire with D = 2.36 nm.

Any physical observable was expressed in terms of the Bogoliubov quasiparticle densities. Therefore dynamics of these quantitates can be expressed in the framework of the density-matrix formalism. The above equations for the particle-like and hole-like quasiparticle amplitudes $u_\chi(\mathbf{r})$ and $v_\chi(\mathbf{r})$ *were* supplemented by the closed set of the Heisenberg equation of motion (EOM) for the averages, like, $\langle \gamma_\chi^+ \gamma_\chi \rangle$, $\langle \gamma_{\bar{\chi}}^+ \gamma_{\bar{\chi}} \rangle$, $\langle \gamma_\chi^+ \gamma_{\bar{\chi}}^+ \rangle$, $\langle \gamma_{\bar{\chi}} \gamma_\chi \rangle$. In the mean field treatment we did not get an infinite hierarchy of equations.

During the investigation we have analyzed the non-equilibrium dynamics of confinement-induced multiband superconductors after a perturbation in the non-adiabatic regime. We limited ourselves to metallic high-quality tin nanowires. In addition, we included in our calculations the confinement-induced spatial variation of the pair condensate. Within the density matrix formalism based on the BCS model/ the Bogoliubov–de Gennes equations we showed (see Fig. 2) that the beating-like pattern in the amplitude of the damped dephased oscillations of the time evolution of the order parameter may be attributed to the intrinsic multiband nature of the nanoscale superconductors. The same beating phenomenon was predicted to be induced in the two-band bulk superconductors.

Acknowledgement: The performed investigation required a large amount of numerical calculations. The cluster computational facilities available at the University of Bayreuth were used for this purpose.

I acknowledge the fruitful collaboration and discussions with A. V. Vagov (Institute of Theoretical Physics III, University of Bayreuth, Germany), M. Zachman (Institute of Theoretical Physics III, University of Bayreuth, Germany), V. M. Axt (Institute of Theoretical Physics III, University of Bayreuth, Germany), P. Kettmann (Institute of Solid-State, University of Muenster, Germany), T. Kuhn (Institute of Solid-State, University of Muenster, Germany).

3.3. Quench dynamics of an ultracold Fermi gas in the BCS regime: Spectral properties and confinement-induced breakdown of the Higgs mode: Ultracold Fermi gases have been the subject of many experimental and theoretical studies during recent years. They provide a unique system to study key concepts of condensed-matter theory. This is because in these systems many parameters such as the particle density, the Fermi energy, the confinement potential, or the interaction strength between the Fermions, which in a solid-state system are typically fixed quantities, can be externally controlled in a wide range. In particular, magnetic-field Feshbach resonances provide the means for controlling the interaction strength between fermions by varying an external magnetic field. The tunability of the *s*-wave scattering length, which is the dominant interaction channel, makes ultracold Fermi gases ideal for exploring different regimes of interacting many-body systems in a single system. This includes the limiting regimes of weakly attracting fermions, which condense into Cooper pairs forming a Bardeen-Cooper-Schrieffer (BCS) phase below a certain temperature T_C, and repulsive dimers formed by two fermions, which can undergo a Bose-Einstein condensation (BEC). These two limiting regimes are separated by the strongly interacting BCS-BEC crossover regime where the scattering length diverges and the system exhibits unitary properties.

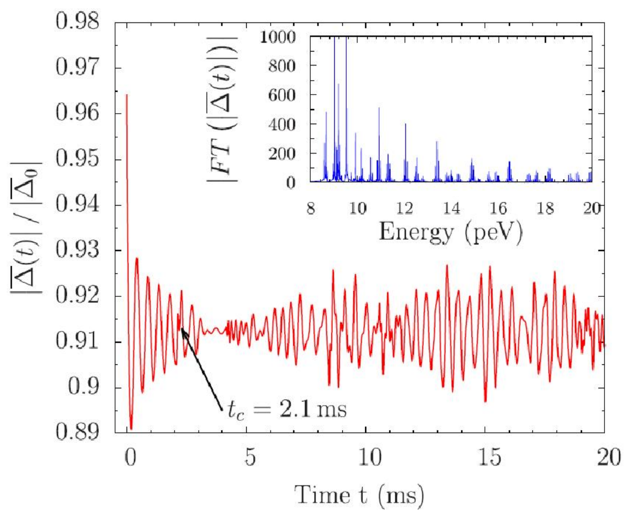

Fig. 3: Dynamics of the spatially averaged gap after a sudden change of the scattering length from −140 to −135 nm (normalized to the spatially averaged ground-state gap of the system before the quench Δ_0|). Inset: Fourier transform of the gap dynamics. The confinement frequencies are $f\perp$ = 11.2 kHz and $f||$ = 240 Hz.

In addition to the variable interaction strength, ultracold atomic gases offer a unique opportunity to explore the influence of a confinement on the pairing correlations, because dimensionality and confinement can be precisely controlled by tuning external parameters. Varying the confinement, which is often well approximated by a harmonic confinement potential, allows one to access new degrees of freedom. Restricting the Fermi gases to quasi-low dimensionality may, e.g., offer the possibility for an experimental evidence of unconventional phases, like the Fulde-Ferrell-Larkin-Ovchinnikov state. Moreover it may help to study and get experimental insight into shape resonances, theoretically predicted for quasi-low-dimensional conventional superconductors. At low atom numbers, the shell structure associated with the filling of individual transverse oscillator states has been observed. On the theoretical side the ground-state properties of a ^{6}Li gas confined in a cigar-shaped laser trap have been investigated predicting size-dependent resonances of the superfluid gap, similar to the case of superconducting nanowires, yielding an atypical BCS-BEC crossover.

An important effort is now devoted to the exploration of the out-of-equilibrium behavior of trapped ultracold atomic Fermi gases and, in particular, to the determination of their dynamical properties. The dynamics has been studied in the normal as well as in the condensed phase, observing second sound and soliton trains, and showing a low-frequency oscillation of the cloud after a change of the system confinement or optical excitation. Furthermore, state-of-the-art technology allows one to change the coupling constant on such short time scales that it is possible to explore the regime where the many-body system is governed by a unitary evolution with nonequilibrium initial conditions. In ultracold atomic Fermi gases the dynamics may be initiated by readjusting the pairing interaction through switching an external magnetic field in the region of a Feshbach resonance (i.e., a quantum quench) or by a rapid change of the confinement potential of the trap. Due to the small energies in the trapping potential the dynamics in the Fermi gases take place on a millisecond time scale. Therefore, in contrast to metallic superconductors, where subpicosecond excitations are required to achieve nonadiabatic dynamics, in atomic gases the nonadiabatic regime can be reached already by excitations in the submillisecond range.

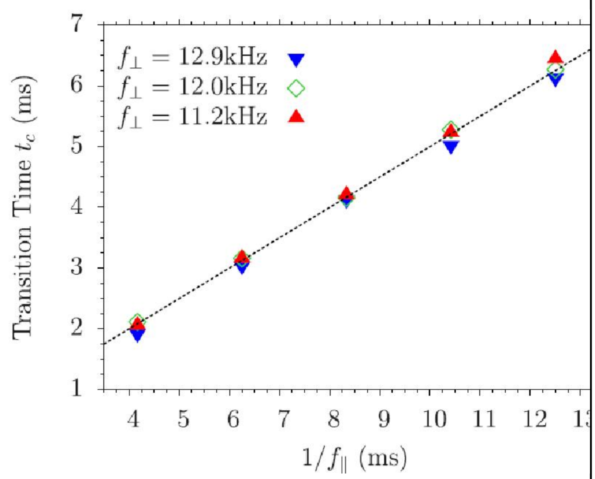

Fig. 4: Transition times of three different perpendicular confinements in dependence of the inverse parallel confinement frequency compared to the prediction from the linearized theory (dashed curve).

In this work we performed a theoretical analysis of the short time BCS dynamics of a ^{6}Li gas confined in a cigar-shaped laser trap. The excitation was modeled by a sudden change of the interaction strength which can be achieved through a Feshbach resonance by an abrupt change of the external magnetic field. Applying the well-known BCS theory in mean field approximation to ultracold Fermi gases we have shown that the change of the coupling strength induces a collective oscillation of the Bogoliubov quasiparticles close to the Fermi level. This results in a damped amplitude oscillation of the BCS gap, which corresponds to the Higgs mode.

We have shown that the amplitude of the spatially averaged gap performs a damped oscillation breaking down after a certain time *tc*, which is determined by the parallel confinement frequency, i.e., by the length of the cloud (see Fig. 3). Afterwards a rather irregular oscillation involving many different frequencies occurs. We have investigated the influence of the confinement on the gap dynamics and the impact of the size-dependent superfluid resonances on its qualitative behavior. It turned out that in the case of a resonant system, i.e., a system where the Fermi energy is close to a sub-band minimum, the dynamics of the order parameter exhibits a strong damping and, for sufficiently long systems, a revival before eventually the irregular regime is reached. In contrast, in an off-resonant system the damping is much less pronounced and the oscillation before the transition to the irregular regime is mainly determined by a single frequency. By analyzing the linearized version of the equations of motion for the quasiparticle excitations we were able to interpret the observed features of the dynamics. It turned out that for the excitations studied in this paper the linearized equations well reproduce the dynamical behavior of the gap, except for some slight details resulting from the nonlinearities in the full equations of motion (Fig. 4). From the linearized model it becomes evident that the system approximately behaves like a set of weakly coupled harmonic oscillators. The frequencies as well as the couplings of these oscillators are completely determined by the system parameters after the excitation while the amplitudes of the different eigenmodes depend on the details of the excitation. The analysis revealed in particular that the transition time to the irregular dynamics is directly related to the energy separation of the one-particle energies while the differences between resonant and nonresonant systems are caused by the different densities of states and coupling efficiencies close to the sub-band minima.

Acknowledgement: The large part of the research was performed in the University of Muenster.

I acknowledge the fruitful collaboration and discussions with V. M. Axt (Institute of Theoretical Physics III, University of Bayreuth, Germany), S. Hannibal and P. Kettmann (Institute of Solid-State, University of Muenster, Germany), T. Kuhn (Institute of Solid-State, University of Muenster, Germany).

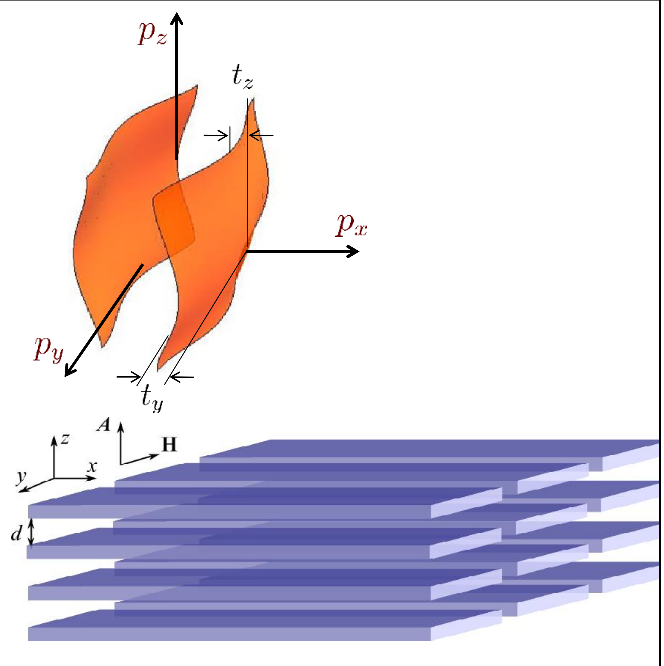

Fig. 5: Scheme of the quasi-1D conductor in a parallel magnetic field.

3.4. Peculiarities of the orbital effect in the FFLO state in quasi-1D SCs: Motivated by the recent experimental findings of clean quasi-one-dimensional compounds with the orbital pair-breaking effect sufficiently weaker than the Pauli paramagnetic limit, we investigate in this work the possibilities of the spatially modulated superconducting phase formation in quasi-1D superconductors with *s*-wave pairing. We consider a quasi-one-dimensional (quasi-1D) conductor with the following electron spectrum (as shown in Fig. 5):

$$E_{\mathbf{p}} = \frac{p_x^2}{2m_x} + 2t_y \cos\left(p_y d_y\right) - 2t_z \cos\left(p_z d_z\right)$$

where d_y and d_z are the interchain distances along the *y*- and *z*-axis, respectively. We assume that the couplings between chains in both directions are small [see Fig.5, i.e. $t_z \ll T_{c0}$ and $t_y \ll T_{c0}$, but sufficiently large to suppress the CDW and SDW transitions, to stabilize the superconducting long-range order and to make the mean field treatment justified, $T_{c0}^2/E_F \ll t_z$, $T_{c0}^2/E_F \ll t_y$. Here T_{c0} is the critical temperature of the system at $H = 0$.

Taking into account that the system is near the second-order phase transition, we can employ the linearized Eilenberger equation for a quasi-1D superconductor in the presence of the magnetic field (in the momentum representation with respect to the coordinate *z*)

$$\left(\Omega_n + \widehat{\Pi}\right) f_\omega\left(x, p_\perp\right) = \left[\Delta\left(x\right) - \frac{f_\omega}{2\tau}\right] \mathrm{sign}\left(\omega_n\right)$$

where

$$\widehat{\Pi} \equiv \frac{\hbar}{2} v_F \frac{\partial}{\partial x} + 2it_z \sin\left(p_z d_z\right) \sin\left(Q_z x\right)$$

The order parameter is defined self-consistently as (*s*-wave)

$$\Delta\left(x\right) = 2\pi T \ \mathrm{Re} \sum_{\omega>0} \left(f_\omega\left(x, p_y, p_z\right)\right)$$

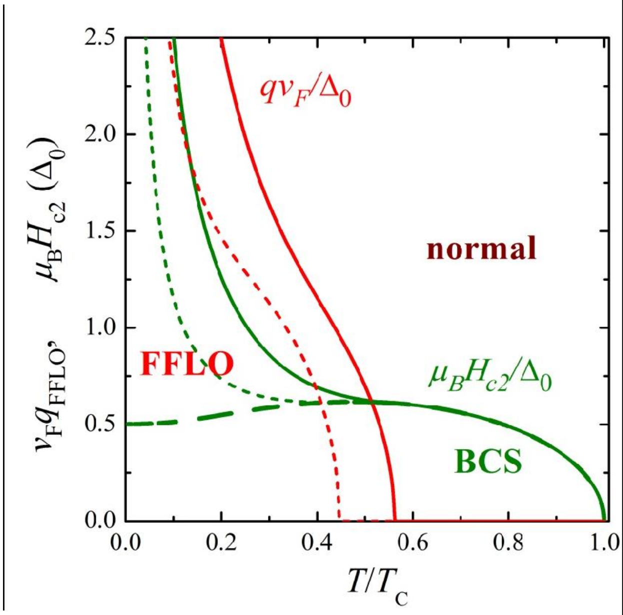

Fig. 6: The temperature dependence of the upper critical field in the Pauli limit and the absolute value of the FFLO modulation vector *q* in quasi-1D superconductors.

We seek the solution of the linearized Eilenberger equation in the form

$$f_\omega\left(x, p_y, p_z\right) = e^{iq_x x} \sum_m e^{imQ_z z} f_m\left(p_y, p_z\right)$$

This expansion takes into account the possibility for the formation of the pairing state with finite center-of-mass momentum. The Eilenberger equation gives

$$T_c = T_{cP} / \left[1 + A\left(S_{\mathrm{O}} - S_{\mathrm{R}}\right)\right]$$

where

$$S_{\mathrm{O}} \equiv t_z^2 \overline{a}_\xi$$

$$S_{\mathrm{R}}^\xi \equiv -\frac{(\overline{a}_\xi - \overline{b}_\xi)t_z^2 - \delta_\xi}{2} - \frac{t_z^2}{2}\sqrt{\left[\overline{a}_\xi - \overline{b}_\xi - \delta_\xi / t_z^2\right]^2 - 4\gamma_\xi^2}$$

Figure 6 illustrates the temperature dependence of the absolute value of the FFLO wave vector **q** (red lines) and the upper critical field (green lines) calculated in the clean limit and when the moderate disorder is taken into account while the orbital corrections are neglected. The magnitude of the **q** vector monotonically increases from zero at the tricritical point until infinity in the clean sample or until some large values depending on the mean-free path while accounting for the disorder. The optimal direction of the modulation vector was found to be along the conducting chain axis. Figure 7 shows the corrections to the transition temperature due to the orbital motion as a function of reduced temperature for different angles that the magnetic field makes from the direction of the conducting chains. In both sides from the tricritical point the system exhibit angle dependence of the onset of superconductivity. In the FFLO phase we see strong deviations between curves for different angles. The dashed and solid curves here are the results for different level of the expansion of the order parameter.

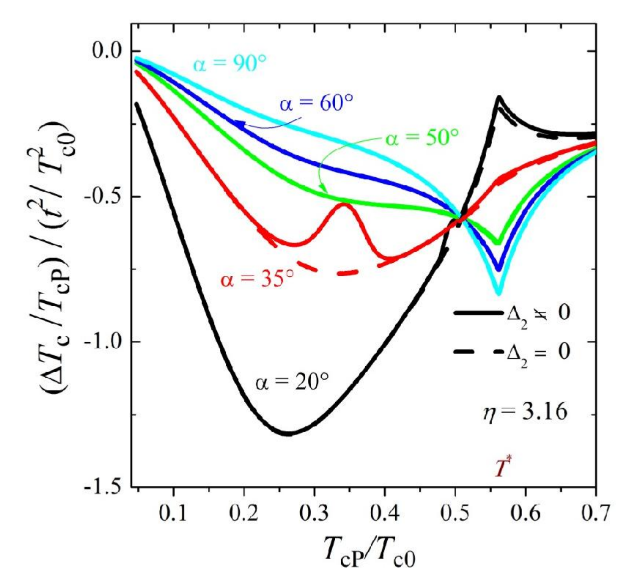

Fig. 7: Orbital correction to the T_{cP}; Contribution of the orbital effect as a function of T_{cP} / T_{c0} for several magnetic field tilting angles θ between **H** and **q.**

In this work we have described the behavior of the quasi-1D superconductors in high magnetic field with different tilting with respect to the principal axis of the compound (see Fig. 7). We demonstrated that (*i*) the experimentally observed in quasi-1D compounds, such as purple bronze Li0.9Mo6O17, the transition-metal-chalcogenide compound Nb2Pd0.81Se5, or 4A carbon nanotubes grown in zeolite crystals, large values of the upper critical field in the fields parallel to the compound principal axis and at low temperature may be attributed to the stabilization of the FFLO superconducting phase (Fig. 6). The low-temperature FFLO phase is characterized by an essential reduction of the magnetic field induced orbital effect as compared to the high-temperature FFLO phase. This makes the *Tc(θ)/TcP* dependence much closer to the paramagnetic FFLO limit. The finite magnitude of the paramagnetic limit may result, for example, from the impurities scattering. (*ii*) We found that the upper critical field is maximal for the modulation vector **q** parallel to the most conducting direction. (*iii*) We demonstrated that in quasi-1D compounds one can explore experimentally all field regimes, from the weak field up to the re-entrant one at high magnetic field, by rotating the magnetic field direction (Fig. 7). The high-field superconductivity survives because the quasi-1D Fermi surface stabilizes the FFLO state that can exist above the Pauli limited fields. (*iv*) The resonance between the modulation vector of the FFLO phase and the vector potential of the magnetic field may lead to anomalous cusps in the field-direction dependence of the upper critical field analogous to those calculated previously in quasi-2D conductors. At the resonance, the interplay between the orbital and paramagnetic effects may result in a lock-in effect. (*v*) We discussed that the inverse effects pertinent to the T^{**} may become an additional tool to evidence the

FFLO state. We suggested that observation of these effects may serve as a direct proof for the appearance the FFLO phase in quasi-1D superconductors. The possibility to experimentally observe the orbital effect in quasi-1D superconductors should provide very reach information about the parameters of the FFLO phase.

*Acknowledgement***:** This work was done analytically and I acknowledge the fruitful collaboration and discussions with A. I. Buzdin (LOMA, University of Bordeaux).

3.5. Resonant tunneling and localized states in a graphene monolayer with a mass gap: This part of the performed research seems stays slightly a part from the rest. However it is much related to some effects in superconductors and as so we consider as a basis step for our further research in the domain of superconductivity of nanoscale samples.

Analysis of single particle scattering is an essential step in describing transport properties of graphene, where the interaction between carriers is typically small and the system is often in the ballistic regime. The problem of a single particle tunneling for the Dirac-like Hamiltonian of graphene leads to many nontrivial properties, not observed in standard quantum mechanics. In particular it gives rise to the Klein tunneling, also known as Landau-Zenner tunneling in the theory of semiconductors, related to transmutation of electrons into holes and vice versa in the scattering process. This type of tunneling can be traced in the conductance or short-noise measurements in ballistic samples. In experiments potential barriers are constructed by inserting charge impurities or by creating terrace steps in the substrate. Tunable barriers are achieved by varying the gate voltage. This allows detailed studies of the effect of barrier shape on the transport and paves the way for the creation of graphene-based devices.

The Achilles heel of graphene application in electronic devices is a vanishing gap in its spectrum. In order to open the gap and, furthermore, to control its value various methods have been proposed. For example, one can apply electrostatic gates or create a superlattice. Recent efforts in material science focused on designing new types of materials by doping graphene and by using boron nitride as a support of graphene sheets. A chemical boron/nitrogen doping opens the way for mass production of the graphene-based field transistors. Obviously carrier scattering and subsequently electric transport in graphene based switching devices depends on the spectral gap, so that the latter has to be taken into account in the theoretical modeling.

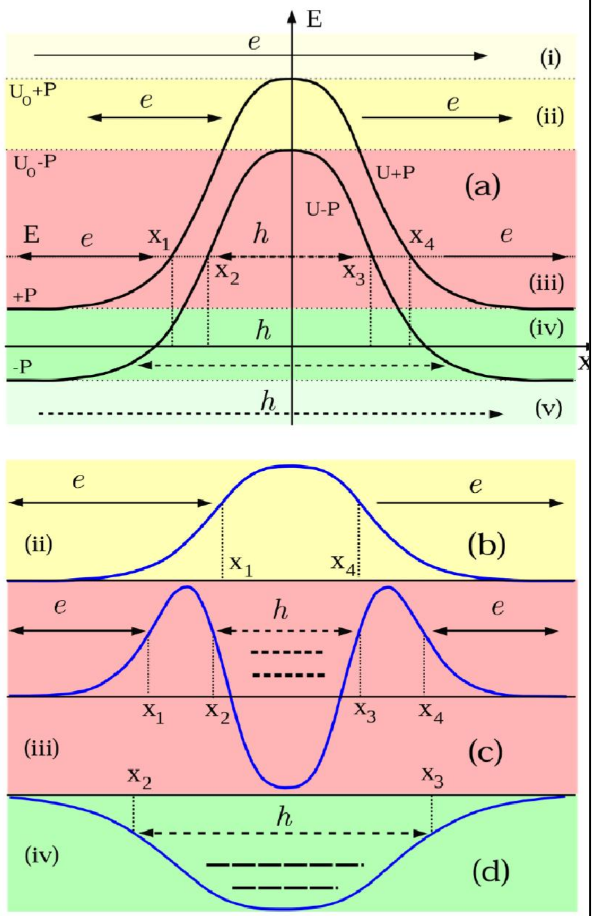

Fig. 8: Different scattering states in intervals (i) – (v), shaded by respective colors, for a single peaked barrier $U(x)$. Continuous black lines in (a) represent the shifted potential $U(x) \pm P$, x_i are turning points found by solving $E = U(x) \pm P$. (b)–(d) Illustrate scattering in energy intervals (ii)–(iv) [shaded by the same colors as in (a)]: (b) Interval (ii) with e-e tunneling of electrons, (c) interval (iii) with the resonant e-h-e tunneling, and (d) interval (iv) with localized h states. e/h denote electrons/holes, blue lines give the effective potential $E^2 - [U(x) - E]^2$, short dashed lines in (c) illustrate positions of virtual hole states, and long dashed lines in (d) represent localized hole states.

Theory description of scattering is most trivial for rectangular or step-like barrier shapes. Despite its simplicity this model is quite useful to illustrate general properties of the Klein-Landau-Zenner tunneling in graphene. However, it cannot capture many physical aspects of the tunneling and is certainly not valid for most experiments, where barriers are typically smooth. For smooth potential profiles the scattering problem is more complicated and significant efforts have been applied to study its various limiting cases. When electrons hit an adiabatically slowly varying potential step the Klein tunneling can exhibit full particle transmission, when scattered in the direction normal to the barrier, or exponentially small transmission, when particles approach the barrier at an angle. Klein tunneling through the barrier with a single maximum can be of a resonant character due to the presence of metastable or evanescent hole states inside the barrier, which then acts in a manner to a Fabry-Perot resonator. Analysis of resonant scattering can be done on a simplified model of a trapezoidal barrier, which has the advantage of being exactly solvable. In a more general case of an arbitrary barrier semiclassical methods can be employed to obtain scattering coefficients as functions of the integral characteristics of the potential that cover many limiting cases. Due to the matrix character of the Dirac equation a derivation of the semiclassical solution can proceed using multiple recipes that are formally different from the conventional WKB method used in quantum mechanics, e.g., using separate Hamiltonians for electron and hole states. A more traditional approach, based on the expansion of the wave function in powers of the Planck constant is also possible, being easier technically and arguably more intuitive physically.

The analog of classical trajectories that appear from the WKB solution of matrix equations, offers a convenient tool for classification of all scattering states associated with the barrier. In particular, it has been used to distinguish fully localized states that are often overlooked in studies of the barrier scattering. An appearance of such states has been discussed earlier only for the rectangular barrier structure that, however, does not lead to a resonating Fabry-Perot structure.

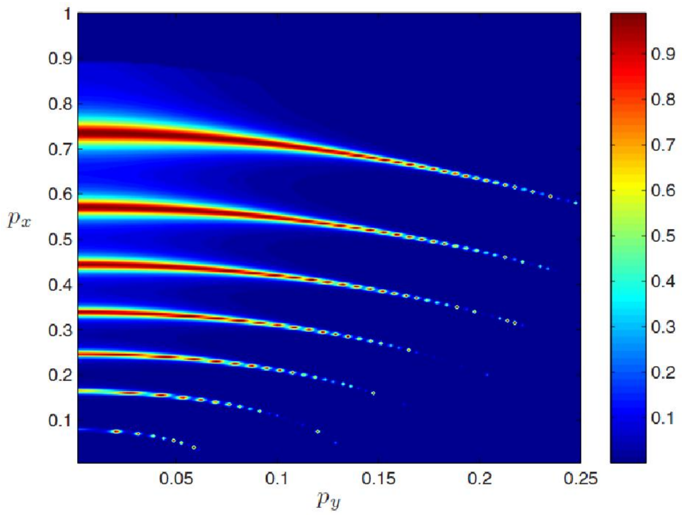

Fig. 9: Bar diagram for the absolute value of the transmission coefficient $|t|^2$ as a function of momentum components p_x and p_y, calculated from the WKB expression for barrier $U = \mathrm{sech}(x)$ for $g = 0.1$. The stripes (red) are the domains of resonant scattering $|t| \approx 1$ that correspond to positions of the virtual states illustrated in Fig. 8.

In this work, having in mind recently obtained graphene based devices with spectral gap, we have presented a semiclassical analysis of scattering on a smooth 1D potential barrier in single layered graphene with a gap. The derivation of the WKB approach follows a standard strategy of expanding the vector wave function in powers of the Planck constant which allows us to explicitly obtain the contributions at each order by solving the corresponding transport equations. We note that a similar approach can also be developed for more complicated systems such as multilayered graphene superconducting structures. Analysis of the scattering on the barrier potential is done within the leading order of the WKB expansion. Using the analog of the classical action several qualitatively different stationary states have been identified, including those of resonant scattering and hole states localized in the vicinity of the barrier. WKB expressions were obtained for the wave functions, transmission coefficients, energies of the resonances and localized states, as well as for the resonance widths (Fig. 8). Apart from the phase factor the expressions obtained in this work have a functional form similar to that derived earlier for the gapless case. However, unlike the latter, the system with nonzero gaps exhibits reflection-less Klein tunneling only at resonances even for the scattering at normal angle (Fig. 9). Positions of the virtual and the localized states are defined by the same Bohr-Sommerfeld-like quantization condition. Unlike standard quantum mechanics, here the number of localized states increases at larger values of the longitudinal momentum component and at larger gap values, so that such states are always present in the system. It was also demonstrated that resonances and localized states can modify the single particle DOS by introducing van Hove singularities. Such states may be important in the electrical transport in the system especially superconducting ones. However, discussion of this aspect is beyond the scope of this work and left for the future research.

*Acknowledgement***:** The large part of the work was done in Krylov Institute and the Loughborough University.

I acknowledge the fruitful collaboration and discussions with A. V. Vagov (Institute of Theoretical Physics III, University of Bayreuth, Germany), V. Zalipaev (Krylov Institute, St. Petersburg, Russia), C. M. Linton (Department of Mathematical Sciences, Loughborough University, Leicestershire, LE11 3TU, United Kingdom)

3.6. Influence of the Landau damping on the on the dynamics of quantum dot coupled to surface phonons: Unique properties of surface plasmon-polariton excitations on nano-scal (SPP) or surface plasmons", promise many interesting applications, in particular, nonclassical light and single-photon sources nano-photonic lasers, meta-materials with non-conventional optical properties, nano-antennas and efficient light sensors, and quantum information devices. Many of them are based on a possibility to achieve effective and precise manipulation of electromagnetic fields using the fact that unlike conventional light SPP modes can resolve scales below the diffraction limit, which can be used to achieve a considerable field enhancement and a better control of its spatial distribution. A standard setback is weak coupling between SPP states and external light which can be corrected by introducing mediating scatters (or emitters) strongly coupled to both light and plasmons. Employing quantum emitters such as strongly confined quantum dots, or superconducting nanograins opens a way for a coherent manipulation of quantum states of the system, which is a prerequisite for quantum information applications. It must be noted, that although SPP excitations involve a macroscopically large number of carriers they can be considered as quantum bosonic field states, with the dynamics induced by discrete creation and absorption of excitation quanta.

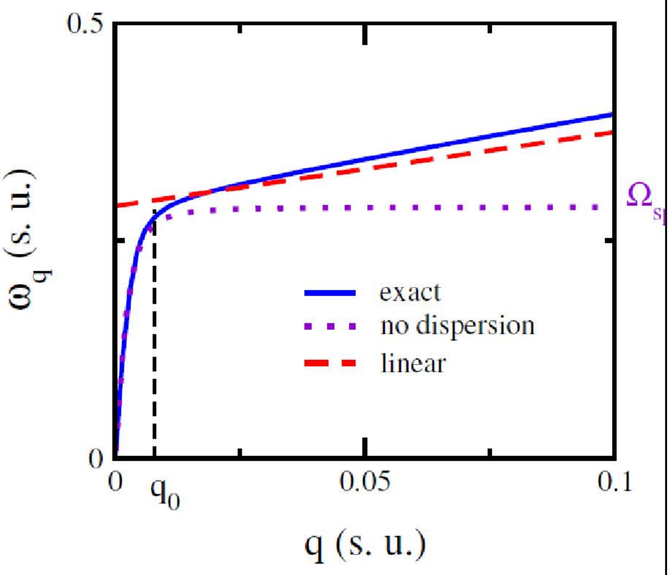

Fig. 10: Real part of SPP frequency dispersion. Continuous (blue) line, labeled “exact", gives the numerical solution. Dotted (violet) line, labeled “no dispersion", is the result obtained for the local approximation for the permittivity. Dashed (red) line, labeled “linear", shows the linear dispersion used in our work.

Description of the dynamics of a quantum emitter in the vicinity of a metallic surface in the regime of strong dynamics must account for quantum coherences. Theoretical modeling can be split into two parts: analysis of SPP excitations and their coupling with the emitter and a subsequent calculation of the dynamics. Such systems belong to a general class of quantum dissipative systems, with SPP playing the role of continua states. Dynamics of such systems is strongly depended on properties of the continuum and thus is sensitive to details of the model and approximations employed in its solution. Ab initio analysis of SPP states, which requires solving Maxwell equations coupled to the microscopic equations for charge carriers in the media, is very complicated so that theoretical studies are typically done with many simplifying assumptions.

A most common approach is a continuous media approximation combined with the linear response theory. This approach separates the material and Maxwell equations; however, solution to the electromagnetic problem is still complicated, especially when the interface between two materials has a non-trivial shape. The electromagnetic problem can be considerably simplified using the assumption the dielectric response is spatially independent (local). This approximation, found in most text-book analysis of SPP states, can be relatively easy extended to any interface geometry. However, this introduces an artificial singularity in the SPP DOS which results in notable changes in the dynamics. For a non-local dielectric response Maxwell equations admit solutions only for few simple cases such as at surface and slabs and, with some reservations, for spheres. Numerical approaches like time-dependent density functional method have been applied recently to describe SPP states beyond the local approximation and in arbitrary geometry. The results demonstrated importance of the non-locality on a nano-size scale. However, extension of those approaches to study a time evolution of SPP modes coupled to a quantum emitter has not been attempted.

This work presents a study of quantum dynamics of a QD, placed in the vicinity of the metallic sample. The dynamics is induced by the coupling between the QD and plasmon-polaritons on the surface of the metal. The calculations are done within the linear approximation for the electromagnetic response, but with the account of the non-locality of the dielectric function of the metal given by the charged degenerate Fermi liquid model (Fig. 10). SPP modes are obtained from the exact solution of the Maxwell equations with the appropriate boundary conditions

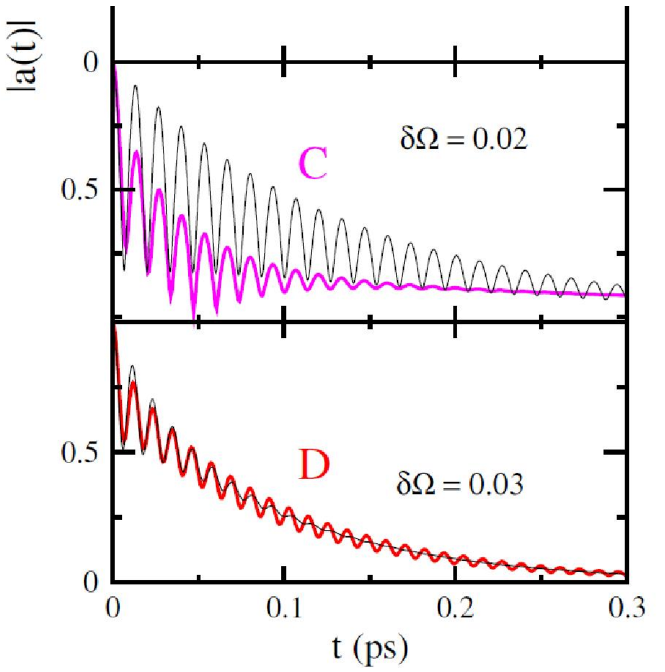

Fig. 11: Examples of the time evolution of the dot.

We have shown that at high wave-vectors the frequency dispersion can be well approximated by the linear dependence which gives a finite group velocity of plasmons. Imaginary part of the velocity appears due to the Landau damping in the Fermi gas of metal charge carriers and defines the decay of plasmon modes. Time evolution of the system is calculated for the initial value problem, which corresponds to the situations when an ultra-short laser pulse initially creates a single exciton in the QD. For this case the Hamiltonian dynamics is calculated exactly, while the decay of SPP modes is accounted for by modifying the memory kernel in the equations of motion for the QD states. The resulting QD time- dependence is defined by analytic properties of the memory kernel, given by the QD-plasmon coupling constants and plasmon frequency dispersion. Obtained results demonstrated that time evolution of the system is a combination of two relaxation processes characterized by two different frequencies and decay rates (Fig. 11). The latter comprise two qualitatively different contributions, due to Landau damping and due to plasmon propagation. The first one yields a smaller rate that corresponds to the long monotonous relaxation. This process can be also described within the Markov approximation, the rate of which estimated from the imaginary type of the dielectric constant. The second rate depends on the kinetic time defined by the group velocity of plasmons and yields a much faster relaxation of Rabi oscillations. It is also demonstrated that when the QD energy is found in the interval of the maximal coupling strength one of the relaxation processes changes from exponential to the power law asymptotic, leading to a much longer visibility of the Rabi oscillations.

The system dynamics is controlled by two main parameters, the detuning and effective coupling strength, that can be effectively parametrized by the QD energy and distance to the QD. The analysis revealed specific power law dependencies on those parameters. Approximations in the calculations are valid when the distance to the QD lies in the interval 5 - 500nm, where the low limit is determined by the non-linearity of dispersion of plasmons while the upper limit is set by the fact that we did not take into account the interaction with delocalized photons. Quantum features of the dynamics are most strongly revealed at distances below 20nm. Although we expect that main conclusions of this work holds at smaller distances. We stress that dynamical features discussed in the work are intimately related to the non-locality of the electromagnetic properties of the metal at nano-scale.

Acknowledgement: I acknowledge the fruitful collaboration and discussions with A. V. Vagov (Institute of Theoretical Physics III, University of Bayreuth, Germany), I. A. Larkin (Institute of Microelectronics Technology Russian Academy of Sciences, 142432 Chernogolovka, Russia)

4. Valorisation/Diffusion (including Publications, Conferences, Seminars, Missions abroad...)

Publications:

Articles in journals with peer review (published):

1. Hannibal S., Kettmann P., Croitoru M. D., Vagov A., Axt V. M., Kuhn T. (2015): Quench dynamics of an ultracold Fermi gas in the BCS regime: Spectral properties and confinement-induced breakdown of the Higgs mode, Physical Review A **91**, 043630, WoS: WOS:000353448500005
2. Shanenko A. A., Aguiar J. A., Vagov A., Croitoru M. D., Milosevic M. V. (2015): Atomically flat superconducting nanofilms: multiband properties and mean-field theory, Superconductor Science and Technology **28**, 054001, WOS:000353015700005
3. Zalipaev V., Linton C.M., Croitoru M. D., and Vagov A. (2015): Resonant tunneling and localized states in graphene monolayer with a mass gap, Physical Review B **91**, 085405, WOS: 000351773900004.
4. Croitoru M. D., Buzdin A.I. (2014): Peculiarities of the orbital effect in the FFLO state in quasi-1D superconductors, Physical Review B **89**, 224506, WoS: 000336975000005.
5. Vagov A., Glässl M., Croitoru M. D., Axt V. M., and Kuhn T. (2014): Competition between pure dephasing and photon losses in the dynamics of a dot-cavity system, Physical Review B **90**, 075309, WoS: 000341258700002.
6. Croitoru M. D., Zachmann M., Vagov A., Axt V. M., Shanenko A. A., Kettmann P., Papenkort T., and Kuh T. (2014): Coherent dynamics of confinement-induced multiband superconductors, Physica C **503**, 183, WoS: 000340070600040
7. Croitoru M. D., Buzdin A.I. (2015): FFLO-wave-vector Lock-in Effect in Quasi-1D Superconductors, Journal of superconductivity and Novel magnetism 28, 1305, WOS:000352085700019.

Articles in journals with peer review (submitted):

8. Croitoru M. D., Shanenko A., Vagov A., Milosevic M., Axt V. M., and Peeters F. (2015): Phonon limited superconducting correlations in metallic nanograins, submitted to Sci.
9. Vagov A, Larkin, A. I. Croitoru M.D. (2015): Influence of the Landau damping on the on the dynamics of quantum dot coupled to surface phonons, in preparation.

Conferences:

10. Croitoru M.D., Vagov A. I. Larkin I. A. (2015): Environment induced changes in noon-adiabatic dynamics od superconductors. In: “Vortex Matter in nanostructured superconductors 2015 – Vortex IX”, Rhodes, Greece, September 13 - September 18 2015, 51. link: http://www.kuleuven.be/inpac/vortex/ (ORAL);
11. Croitoru M. D. (2015): Environment induced changes of superconducting characteristics in nanograins, In: International Conference “Superstripes - 2015”, Ischia – Italy, June 13 - June 18 2015, 67. Link: http://www.ricmass.eu/index.php?option=com_content&view=article&id=92&Itemid=119, (INVITED)
12. Croitoru M. D. (2015): Non-adiabatic dynamics of superconducting pairing in systems with shallow bands, In: International symposium “Nanophysics & Nanoelectronics” Nizhny Novgorod, Russia – March 10-14, 2015, 36, (INVITED);
13. Croitoru M. D. (2014): Peculiarities of the orbital effect in the FFLO state in quasi-1D superconductors, In: International Conference “Superstripes - 2014”, Erice - Sicily, July 25 - July 31 2014, 67. Link: http://www.ricmass.eu/index.php?option=com_content&view=article&id=92&Itemid=119 (INVITED);
14. Croitoru M. D. (2014): Coherent Dynamics of Superconducting Pairing in Multiband Systems, In: 2th International conference MultiSuper, Camerino, Italy, June 23 - June 28 2014, 121. link: http://www.multisuper.ml1.net/ (ORAL);

15. Croitoru M. D. (2014): Coherent Dynamics of Superconducting Pairing in Systems with non-trivial DOS, In: 4th International conference on Superconductivity and Magnetism, Antalya, Turkey, April 27 - May 2 2014, 51. link: http://icsm2014.org/ (ORAL);

16. Croitoru M. D., Buzdin A.I. (2014): Peculiarities of the orbital effect in the FFLO state in quasi-1D superconductors, In: International Workshop "Past and Future Discoveries in Condensed Matter Physics", Bordeaux, March 31 - April 2 2014, (INVITED).

17. Croitoru M.D., Zachmann M., Vagov A., Shanenko A., Axt V.M., Papenkort T., and Kuhn T. (2013): Coherent dynamics of pairing in superconductors with a non-trivial DOS. In: "Vortex Matter in nanostructured superconductors 2013 – Vortex VIII", Rhodes, Greece, September 21 - September 26 2013, 51. link: http://www.kuleuven.be/inpac/vortex/ (ORAL);

Seminars:

18. Croitoru M. D. (2015): Resonance in-plane magnetic field effect in FFLO state in layered superconductors, In: Seminar, University of Camerino, Italy, July 22, 2015;

19. Croitoru M. D. (2014): Superconducting correlations in metallic nanograins coupled to a phonon bath, In: Seminar, University of Bayreuth, Germany, December 12, 2014;

Missions abroad: Scientific visits from the University of Antwerp:

1. Croitoru M. D. (2015): University of Camerino, Italy, July 21 – August 2, 2015;

2. Croitoru M. D. (2014): University of Bayreuth, Germany, December 14 – December 17, 2014.

Scientific visits to the University of Antwerp in relation to the current project:

3. Larkin I. A. (January 11 – 12, 2015), Seminar: "Dynamics of quantum dot coupled to surface phonons", University of Antwerp.

4. Vagov A. (May 28 – June 2, 2015), Seminar: "Multiband superconductors", University of Antwerp.

Future conferences:

20. Croitoru M. D. (2016): Phonon limited superconducting correlations in metallic nanograins, In: 5th International conference on Superconductivity and Magnetism, Fethiye, Turkey, April 24 - 30 2016, link: http://icsm2016.org/ (INVITED);

21. Croitoru M. D. (2016): Environment induced changes of superconducting characteristics in nanograins, In: International Conference "Superstripes - 2016", Ischia – Italy, June 23 - June 28 2016, http://www.ricmass.eu/superstripes/ (INVITED).

22. Croitoru M. D. (2016): The orbital effect in the FFLO state in quasi-low dimensional superconductors, In: International Workshop on quasi-low dimensional superconductors, Natal - Brazil, July 20 - September 10 2016 (INVITED).

23. Croitoru M. D. (2016): The orbital effect in the FFLO state in quasi-low dimensional superconductors, In: International Conferrence on the SF structures, Dresden - Germany, May 20 - May 26 2016 (INVITED).

5. Future prospects for a permanent position in Belgium

I hope to find a position in a Belgian University or a research Institute. However, currently, I am registered as a workless person with VDAB from 01.09.2015.

6. Miscellaneous

I am grateful to Prof. F. M. Peeters, the head of the CMT research group at the University of Antwerp, for hosting my BELSPO grant.

I thank Mrs. Veronique Van Herck for helping me with the administration of the BELSPO project.

I acknowledge the Alexander von Humboldt grant and the Institute of the Theoretical Physics III of the University of Bayreuth, which allowed me to perform large numerical calculations by making use of the

cluster computational facilities available at the University of Bayreuth: MEGWARE computer, Intel Xeon E5520, 1136 processors, 142 nodes, 3.4 TB storage.

The extension of the Problem 3.1 will be investigated by the PhD student of the CMT group dhr. Sam Roelants.

External collaborations: A. I. Buzdin (LOMA, University of Bordeaux), V. Vagov (Institute of Theoretical Physics III, University of Bayreuth, Germany), I. A. Larkin (Institute of Microelectronics Technology Russian Academy of Sciences, 142432 Chernogolovka, Russia), V. Zalipaev (Krylov Institute, St. Petersburg, Russia), C. M. Linton (Department of Mathematical Sciences, Loughborough University, Leicestershire, LE11 3TU, United Kingdom), A. A. Shanenko (University of Pernambuco, Brazil), V. Z. Kresin Lawrence Berkeley National Laboratory, Berkeley, CA USA), V. N. Gladilin (Catholic University of Leuven, Belgium), S. N. Klimin (University of Antwerp, Belgium), M. Zachman (Institute of Theoretical Physics III, University of Bayreuth, Germany), V. M. Axt (Institute of Theoretical Physics III, University of Bayreuth, Germany), P. Kettmann (Institute of Solid-State, University of Muenster, Germany), T. Kuhn (Institute of Solid-State, University of Muenster, Germany), S. Hannibal (Institute of Solid-State, University of Muenster, Germany).

Financial part related to the performed research:

Since it was allowed to use monetary means related to the BELSPO grant for scientific conferences, visits, and missions abroad, please find below the description of the expenses I have made during the BELSPO project (more details, I expect to be provided by the corresponding department of the University of Antwerp).

Conference costs:

Nr.	Conference title	Cost (Euro)
1	"Vortex Matter in nanostructured superconductors 2013 – Vortex VIII", Rhodes, Greece, September 21 - September 26 2013	1256.44
2	International Workshop "Past and Future Discoveries in Condensed Matter Physics", Bordeaux, March 31 - April 2 2014	212.89
3	4^{th} International conference on Superconductivity and Magnetism, Antalya, Turkey, April 27 - May 2 2014	1618.24
4	2^{th} International conference MultiSuper, Camerino, Italy, June 23 - June 28 2014	1000.42
5	International Conference "Superstripes - 2014", Erice - Sicily, July 25 - July 31 2014	1322.57
6	International symposium "Nanophysics & Nanoelectronics" Nizhny Novgorod, Russia – March 10-14, 2015	1085.23
7	International Conference "Superstripes - 2015", Ischia – Italy, June 13 - June 18 2015	1.584.91
8	"Vortex Matter in nanostructured superconductors 2015 – Vortex IX", Rhodes, Greece, September 13 - September 18 2015	843.48
	Total Conferences	**8924.18**

Missions abroad and scientific visits related to the performed research:

Nr.	Mission title	Cost (Euro)
1	Croitoru M. D. (2015): University of Camerino, Italy, July 21 – August 2, 2015	1.858.67

2	Croitoru M. D. (2014): University of Bayreuth, Germany, December 14 – December 17, 2014	493.00
3	Larkin I. A. (January 11 – 12, 2015), Seminar: “Dynamics of quantum dot coupled to surface phonons”, University of Antwerp.	267.39
4	Vagov A. (May 28 – June 2, 2015), Seminar: “Multiband superconductors”, University of Antwerp	778.86
	Total missions	**3397.92**

Other expenses related to the current BELSPO project (equipment, books, overheads, salary, reallocation monetary means, etc.) will be explained directly by the related department of the University of Antwerp.

Online vragenlijst

1. De kenmerken van een terugkeermandaat
Geef op in welke mate u het eens bent met de volgende uitspraken hieronder.

1. Helemaal oneens
2. Eerder oneens
3. Noch eens, noch oneens
4. Eerder eens
5. Helemaal eens
6. Geen mening

a. De weddeschaal is aanvaardbaar

○ 1 ○ 2 ○ 3 ● 4 ○ 5 ○ 6

b. De forfaitaire reistoelage is toereikend

○ 1 ○ 2 ○ 3 ○ 4 ● 5 ○ 6

c. De werkingskosten dekken het grootste deel van de onderzoeksbehoeften

○ 1 ○ 2 ○ 3 ○ 4 ● 5 ○ 6

d. 24 maanden volstaan om zich in België te re-integreren

○ 1 ○ 2 ● 3 ○ 4 ○ 5 ○ 6

e. Het kandidaatsformulier is gemakkelijk in te vullen

○ 1 ○ 2 ○ 3 ○ 4 ● 5 ○ 6

f. Zich kandidaat stellen zou uitsluitend via elektronische weg moeten gebeuren

○ 1 ○ 2 ○ 3 ○ 4 ● 5 ○ 6

g. De terugkeermandaten zijn meer dan bekend in academische kringen

○ 1 ○ 2 ○ 3 ○ 4 ● 5 ○ 6

h. Ik kende de terugkeermandaten lang voor ik mij kandidaat heb gesteld

○ 1 ○ 2 ○ 3 ● 4 ○ 5 ○ 6

i. De oproepen voor kandidaatstelling krijgen voldoende publiciteit

1 2 3 4 5 6

j. De beschikbare informatie tijdens de oproep voor kandidaten is toereikend

1 2 3 4 5 6

k. De informatie tijdens het verloop van het mandaat is relevant

1 2 3 4 5 6

l. De informatie over het selectieproces is correct

1 2 3 4 5 6

m. De lengte van het selectieproces is correct

1 2 3 4 5 6

n. Het selectieproces is doorzichtig

1 2 3 4 5 6

o. De aanvragen van de onderzoekers worden snel verwerkt

1 2 3 4 5 6

p. De met de mandaten belaste personen bij Wetenschapsbeleid staan altijd paraat

1 2 3 4 5 6

q. Het initiatief van de terugkeermandaten moet worden behouden

1 2 3 4 5 6

r. De terugkeermandaten overlappen andere Belgische initiatieven

1 2 3 4 5 6

2. Van terugkeermandaten wordt verwacht dat zij onderzoekers helpen een stabiele plaats te veroveren in België.

a. Hebt u een einde gemaakt aan uw mandaat VOOR de afloop van de periode van 24 maanden

Ja Neen

Was dat om een permanente/vaste plaats te bekleden?

Ja Neen

b. Hebt u nu een permanente/vaste plaats?

Ja Neen

- in België

Ja Neen

- in Europa

Ja Neen

c. Zo ja, volgde die permanente plaats onmiddellijk op het (volledig doorlopen of afgebroken) terugkeermandaat?

Ja Neen

d. Heeft het terugkeermandaat u op welke manier ook geholpen om die permanente plaats te verkrijgen?

Ja Neen

3. Gebruik van het terugkeermandaat

Hoe hebt u de terugkeermandaten leren kennen?

Ik heb de terugkeermandaten leren kennen van de collegas.

b. Hebt u al een dossier voor een onderzoeker ingediend of een collega geholpen?

Ja Neen

c. Zou u een terugkeermandaat aan een onderzoeker/collega aanbevelen?

Ja Neen

d. Zou u van een terugkeermandaat gebruikmaken om een onderzoeker van uw laboratorium/departement naar België te doen terugkeren?

Ja Neen

e. Moet het Federaal Wetenschapsbeleid de resultaten van het in het kader van de terugkeermandaten verrichte onderzoek valoriseren?

Ja Neen